ELSEVIER

Journal of Hydrology 212–213 (1998) 213–229

Journal of Hydrology

A remote sensing surface energy balance algorithm for land (SEBAL)
2. Validation

W.G.M. Bastiaanssen[a,*], H. Pelgrum[a], J. Wang[b], Y. Ma[b], J.F. Moreno[c], G.J. Roerink[a], T. van der Wal[a]

[a]*DLO-The Winand Staring Center for Integrated Land, Soil and Water Research (SC-DLO), P.O. Box 125, 6700 AC, Wageningen, The Netherlands*

[b]*CAS-Lanzhou Institute of Plateau Atmospheric Physics, 316 Dong-gang Xi-lu, Lanzhou, Gansu 730000, P.R. of China*

[c]*University of Valencia, Faculty of Physics, Department of Thermodynamics, Campos de Burjassot, 46100 Valencia, Spain*

Abstract

The surface fluxes obtained with the Surface Energy balance Algorithm for Land (SEBAL), using remote sensing information and limited input data form the field were validated with data available from the large-scale field experiments EFEDA (Spain), HAPEX-Sahel (Niger) and HEIFE (China). In 85% of the cases where field scale surface flux ratios were comparedwith SEBAL-based surface flux ratios, the differences were within the range of instrumental inaccuracies. Without any calibration procedure, the root mean square error of the evaporative fraction \Delta (latent heat flux/net available radiation) for footprints of a few hundred metres varied from $\Lambda_{RMSE} = 0.10$ to 0.20. Aggregation of several footprints to a length scale of a few kilometres reduced the overall error to five percent. Fluxes measured by aircraft during EFEDA were used to study the correctness of remote sensed watershed fluxes (1,000,000 ha):The overall difference in evaporative fraction was negligible. For the Sahelian landscape in Niger, observed differences were larger (15%), which could be attributed to the rapid moisture depletion of the coarse textured soils between the moment of image acquisition (18 September 1992) and the moment of in situ flux analysis (17 September 1992). For HEIFE, the average difference in SEBAL estimated and ground verified surface fluxes was 23 W m^{-2}, which, considering that surface fluxes were not used for calibration, is encouraging. SEBAl estimates of evaporation from the subsealevel Qattara Depression in Egypt (2,000,000 ha) were consistent with the numerically predicted discharge from the groundwater system. In Egypt's Nile Delta, the evaporation from a distributed field scale water balance model at a 700,000 ha irrigated agricultural region led to a difference of 5% with daily evaporative fluxes obtained from SEBAL. It is concluded that, for all study areas in arid zones, the errors average out if a larger number of pixels is considered. Part 1 of this chapter deals with the formulation of SEBAL.

Keywords: Surface fluxes, validation, remote sensing

1. Introduction

Due to the limited technical and financial means available for measurements of natural variations in surface fluxes over heterogemeous land surfaces, the performance of remote sensing flux algorithms cannot be straightforwardly assessed. Sometimes, surface flux maps estimated by the use of remote sensing algorithms have not been verified at all (e.g. Gurney

* Corresponding author. Corresponding address. ITC, P.O. Box 6, 7500 AA, Enschede, The Netherlands.

0022-1694/98/$ - see front matter
PII: S0022-1694(98)00254-6

and Hall, 1983; Ottle et al., 1989; Smith and Choudhury, 1990). Diak (1990) determined regional fluxes from radio soundings, which provide useful information on the bulk exchange processes of complex landscapes that can be used to calibrate regionally averaged surface energy balances estimated from remote sensing data. Such data sets are, however, less suitable for validating field scale fluxes. In ideal situations, surface fluxes should be measured in situ and simultaneously on all dominant land use types. Taconet et al. (1986) and Kustas et al. (1990) used three to four stations to validate their meso scale surface flux map, trading off between what was required and what was technically and financially feasible for a relatively small team of scientists and technicians. The availability of data from large-scale field experiments held over the last ten years should be considered the best option for verifying the regional surface energy balance estimated from remote sensing data. Examples are given for FIFE (Sellers and Hall, 1992), EFEDA (Bastiaanssen et al., 1997) and HAPEX-Sahel (Chehbouni et al., 1997).

Evaporation values from remote sensing data can also be validated with regionally calibrated water balances. Hydrological models are classically calibrated against time series of pressure heads, soil moisture and surface runoff. The present paper assesses and summarizes the potential of several procedures to validate remote sensing algorithms in a range of landscapes and climates. Case studies in different agro-ecosystems were used to reveal how the accuracy of SEBAL changes with the spatial scale and the type of landscape. The validation procedures tested include:

1. Turbulent surface fluxes measured in the field;
2. Airborne turbulent flux measurements;
3. Soil moisture profiles measured in the field;
4. Hydrological models.

2. Validation by the means of turbulent surface fluxes measured in the field

2.1. Footprint issues

Field measurements of turbulent surface fluxes by means of instrumented towers are representative of a relatively small source area, viz. the footprint with length x in the upwind direction which contributes to the establishment of a certain flux. The measured flux F_0 relates to the orientation and length of this footprint in the upwind direction, which vary with the height above the surface at which the fluxes are measured, z_{meas}, as well as with surface parameters such as the surface roughness z_{0m}, the displacement height d, and wind variables such as speed u and direction (e.g. Itier et al., 1994). Schuepp et al. (1990) showed analytically that the contribution to the measured flux of land surface elements adjacent to the tower is significantly higher than that from land surface elements located at a greater distance (x) from the tower:

$$\frac{\int F_0(x)\,\mathrm{d}x}{F_0} = \exp\left(-\frac{u_{avg}}{u_*}\frac{z_{meas}}{kx}\right)(-) \quad (1)$$

where $\int F_0(x)\mathrm{d}x/F_0$ represents the cumulative flux at a distance x relative to a flux measurement at height z_{meas} representing a spatially constant flux and u_* (m s^{-1}) is the friction velocity. Eq. (1) is a tool for integreating the pixel wise fluxes in a non-linear fashion in such a way that they become compatible with tower-based fluxes. The average wind speed u_{avg} of the profile to with u_* applies (see Eq. 1) can be calculated from:

$$u_{avg} = u_* \frac{\ln(z_{meas}/z_{0m}) - 1 + z_{0m}/z_{meas}}{k(1 - z_{0m}/z_{meas})}\ (\mathrm{m\ s^{-1}}) \quad (2)$$

Unless the landscape is strictly uniform, the exact field orientation and the wind direction of the source areas is crucial for validating pixel wise surface fluxes. Although it is felt that the aspect of non-linear flux integration is crucial in validation studies, most studies have ignored this issue: pixel-based fluxes have been compared directly with tower-based flux measurements without considering footprint aspects. Preferably, the pixel size should be a small fraction of the footprint, so that the areal integration pixel wise $F_0(x)$ values can be obtained according to their distance from the pixel on which the tower is located. Validation of low resolution flux maps with pixels larger than the footprint requires a nested calibration procedure between tower-based fluxes, high resolution surface flux maps and low resolution flux maps (Fig. 1).

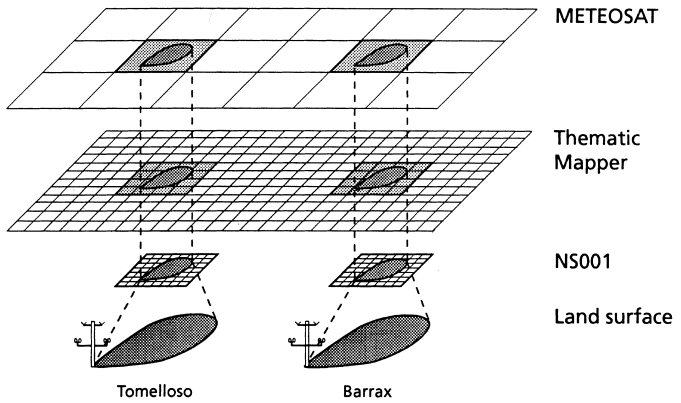

Fig. 1. Multi-scale validation procedure required for the verification of remote sensing-based surface flux maps with different spatial resolutions. The NS001 is a Daedalus AAD1268 twelve channel multi-spetral scanner mounted on an aircraft.

2.2. NS001 measurements of the Barrax and Tomelloso super-sites (EFEDA)

A plateauthreatened by land degradation between 2°–3°30′W and 39°–40° N in Central Spain was selected for an in-depth analysis of water and energy balances during EFEDA (Fig. 2). The EFEDA study area consists of three super-sites, situated at distances of 70 km from one another: the dry farming area of Tomelloso, the irrigated area of Barrax and the hilly Rada de Haro areas where agriculture is only marginally feasible (Bolle et al., 1993). A joint field programme was organised to conduct simultaneous field scale flux measurements. Surface fluxes were measured at 21 stations, most of which were located at the Tomelloso super-site.

During the airborne NS001 mission on June 29 (1991), visible and infrared measurements were made from flying altitude. The NS001 pixel size was 18.5 m, which is suitable for footprint and integration. As a consequence of irrigation practices, The Barrax region is characterised by a patchy type of agriculture, with a mixture of rainfed and irrigated fields (see Fig. 11). The validation of the SEBAL-based fluxes is demonstrated in Fig. 3. A total of 13 individual flux towers were used for this purpose. Most of the stations (10) were situated 5 to 15 km east of Tomelloso. The Barrax stations (3) were situated at La Gineta, 5 km east of the Barrax village.

The H and λE fluxes measured in situe by the EFEDA participants had different integration times. Since H changes almost continuously with the solar elevation, the instantaneous remote sensing based H-flux could not be compared with half-hourly or hourly integrated H-fluxes. To overcome this inconsistencies, the evaporative fraction (see Eq. 3) was computed (Table 1). Experimental evidence indicates that for homogeneous (Shuttleworth et al., 1989) and heterogenous land surfaces, Λ, is temporarily stable between 1000 and 1500 hours local time (Bastiaannssen et al., 1996). The evaporative fraction has therefore been selected as a basis to validate the instantaneous surface energy balance.

$$\Lambda \frac{\lambda E}{Q* - G_0} = \frac{\lambda E}{\lambda E + H} \ (-) \tag{3}$$

The turbulent surface fluxes at the 13 stations were measured using eddy correlation, Bowen-ratio and flux profile-energy budget methods. The H and λE fluxes measured in the field have an error due to instrument uncertainty and calculation procedures to obtain fluxes. In accordance with the technique applied to measure H and λE, the error orginating from inaccurate H and λE fluxes and propagated into Λ was computed for each station. The allocation of the pixels in the surroundings of the tower affecting the in-situ flux was done using the theories incorporated in Eq. (1). In the absence of sufficiently accurate data on u_*, d, u and z_{0m} on June 29, it was impossible to calculate the 13 different footprints. hence Eq. (1) could not be applied. Two rectangular integration regions of (i) 5*5 and (ii) 7*13 pixels were chosen

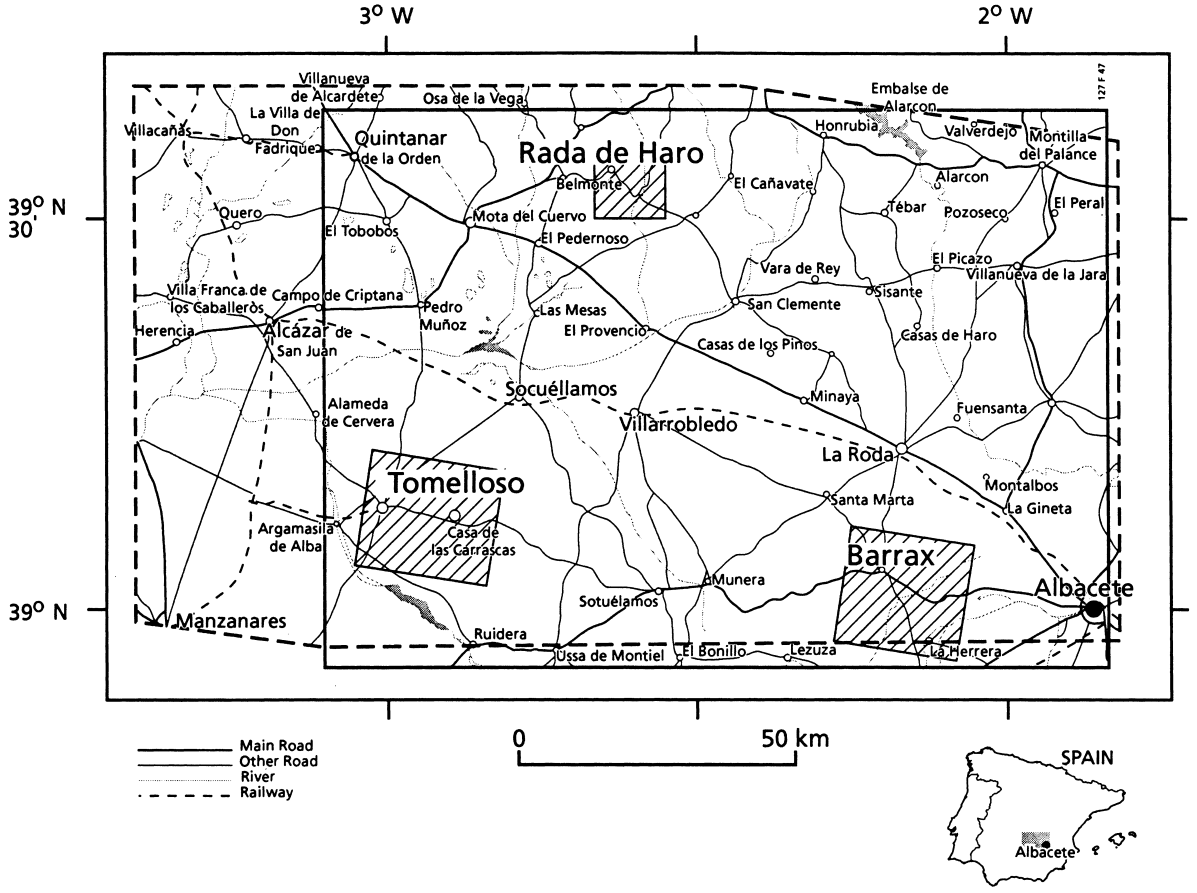

Fig. 2. Location of the EFEDA grid in Castilla la Mancha, Central Spain. The Barrax, Tomelloso and Rada de Haro super-sites are indicated.

instead, and all pixels were given equal weight. This is not correct, but it was one option to include the available flux data in the validation procedure. It was concluded that all towers in Fig. 3, without exception, lie within an envelope of one times the standard deviation. Using the centre of each error bar, the root mean square error became $\Lambda_{RMSE} = 0.10$. The slope of the fitted line for 5*5 pixels was 0.997 ($R^2 = 0.79$) while 7*13 pixels induced a clear cut shift in the slope of 1.488 ($R^2 = 0.76$). Table 1 shows that the selection of the size of the footprint (25 or 91 pixels) had consequences mainly for flux stations 4 and 10. The significant deviation of station 4 from the 1:1 line is purely related to the selection of the integration pixels. Station 5 (CNRM-2) tended to have a poor performance regardless of the footprint selected.

2.3. Landsat thematic mapper measurements at Castilla la Mancha (EFEDA)

EFEDA's ultimate goal was the development of a set of techniques to assess the bulk surface energy balance at grid square scale of numerical atmospheric models. Since a Thematic Mapper image covers 100% of the EFEDA-grid, SEBAL was executed from the cloud free overpass on June 12. Terrain elements comprising agricultural crops and natural vegetation, which were not the subject of intensive field research during the Special Observation Period (SOP), could in this way be incorporated in the determination of the regional surface energy balance. The evaporative fraction based on TM data was validated against in-situ flux data (Fig. 4). Again, 13 flux towers could be

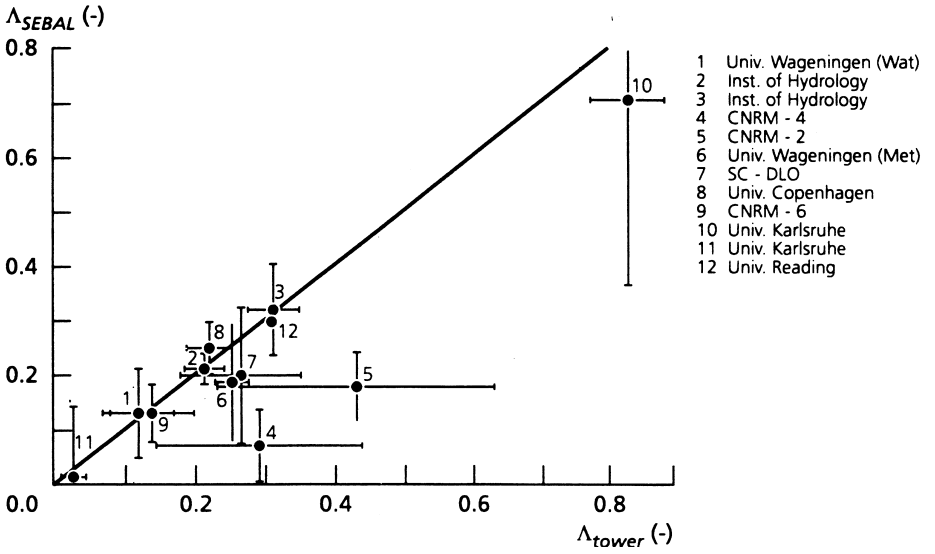

Fig. 3. Validation of the SEBAL-derived evaporative fractions, \Lambda SEBAL, against tower measurements of evaporative fractions, Λ_{tower} for June 29, 10 21′ GMT, 1991 (NS001). Error bars are indicated. EFEDA participants are indicated by number. The footprint of each flux tower is 92.5*92.5 m^2.

Table 1
Data on evaporative fraction derived using the SEBAL parameterization and *in-situ* tower measurements collected by various EFEDA participants during the Special Observation Period. The values between brackets are the standard deviations of the areally integrated at-pixel values (in the case of SEBAL) or standard measurement errors (in the case of tower data), NS001. 10:21 h GMT, June 289, 1991. Flux stations 9, 10 and 11 are situated in Barrax. The other stations were set up in Tomelloso

Institution	Land use	Coordinates UTM	Ground-based Λ-values	SEBAL 25 pixels	SEBAL 91 pixels
Wageningen Univ. (Wat)	Fallow	508919.50, 4333460.00	0.12 (0.06)	0.14 (0.08)	0.17 (0.09)
Inst. of Hydrology	Vetch	504440.39, 4333523.69	0.21 (0.03)	0.22 (0.04)	0.20 (0.06)
Inst. of Hydrology	Vineyard	509309.50, 4333010.00	0.31 (0.04)	0.33 (0.08)	0.30 (0.13)
CNRM-4	Vetch	504089.50, 4333580.00	0.29 (0.15)	0.08 (0.07)	0.17 (0l24)
CNRM-2	Vineyard	506309.50, 4332350.00	0.43 (0.21)	0.19 (0.06)	0.17 (0.07)
Wageningen Univ (Met)	Vineyard	506009.50, 4332290.00	0.25 (0.03)	0.20 (0.11)	0.21 (0.10
DLO Winand Staring Centre	Vineyard	505859.50, 4332320.00	0.26 (0.09)	0.21 (0.12)	0.20 (0.11)
Copenhagen University[a]	Vineyard	506399.50, 4330940.00	0.22 (0.03)	0.26 (0.05)	0.25 (0.06)
CNRM-6	Fallow	576989.50, 4325240.00	0.14 (0.07)	0.14 (0.05)	0.14 (0.05)
Karlsruhe University	Maize	575129.50, 432070.00	0.82 (0.10)	0.72 (0.36)	0.54 (0.44)
Karlsruhe University	Fallow	575039.50, 4324460.00	0.03 (0.01)	0.02 (0.13)	0.09 (0.13)
Reading University[a]	Vineyard	509249.50, 4333250.00	0.31 (–)	0.31 (–)	0.31 (–)
Reading University[a]	Vetch	504299.50, 4333580.00	0.28 (–)	0.25 (–)	0.25 (–)

[a] For June 28, taken from Bolle and Streckenbach, 1992

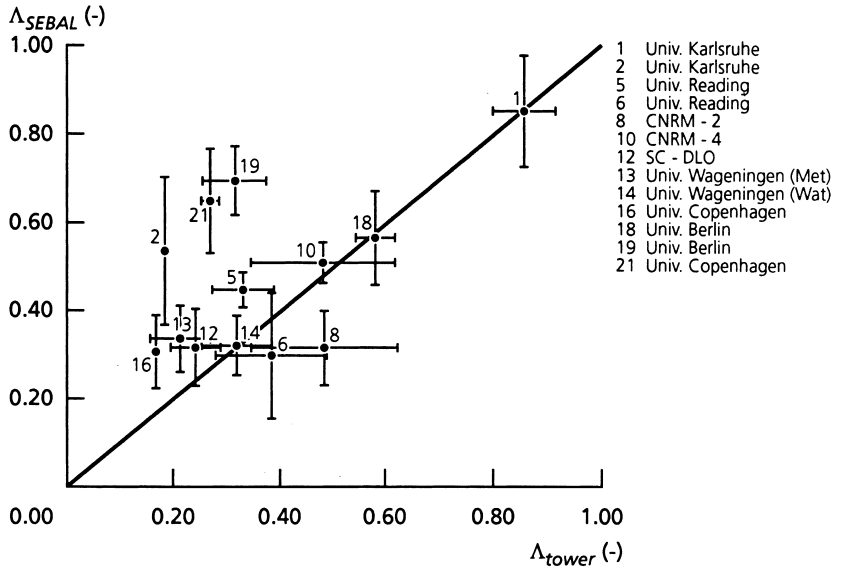

Fig. 4. Validation of the SEBAL-derived evaporative fractions, Λ SEBAL, against tower measurements of evaporative fractions, Λ tower for June 12, 12, 10:12 h GMT, 1991 (Thematic Mapper). Error bars are indicated. EFEDA participants and indicated by number. The footprint of each flux tower was calculated by means of Eq. (1).

included in the comparison,although they were not the same towers as presented in Fig. 3 (see Table 2). The footprints for the selection of the pixel-fluxes to be areally integrated were calculated according to the guidelines provided by Eq. (1). In this calculation, the left hand side of Eq. (1) represents the aggregated flux from heterogeneous terrain, assuming that the theory holds for such terrain The total horizontal distance in the upwind direction for which the cumulative flux contribution is approximately 100% was

Table 2
Data on evaporative fraction derived with the SEBAL parameterization and in-situ tower measurements collected by various EFEDA participants during the Special Observation Period. The values between brackets are the standard deviations of the areal integrated at-pixel values (in the case of SEBAL), or standard measurement errors (in the case of tower data), Landsat Thematic Mapper, 10:12 h GMT, June 12, 1991. Flux stations 1 and 2 were near Barrax, 18, 19 and 21 at Rada de Haro and the remaining stations were set up at the Tomelloso super-site

Institution	Land use	Coordinates UTM	Ground-based Λ-values	SEBAL Schuepp method
Karlsruhe University	Maize	575129.50, 4324070.00	0.86 (0.10)	0.85 (0.57)
Karlsruhe University	Fallow	575039.50, 4324460.00	0.19 (0.02)	0.54 (0.23)
Reading University	Vetch	504299.50, 4333580.00	0.33 (0.11)	0.45 (0.07)
Reading University	Vineyard	509249.50, 4333250.00	0.39 (0.20)	0.30 (0.22)
CNRM-2	Vineyard	506309.50, 4332350.00	0.48 (0.25)	0.32 (0.19)
CNRM-4	Vetch	504089.50, 4333580.00	0.48 (0.25)	0.51 (0.05)
DLO Winand Staring Centre	Vineyard	505859.50, 4332320.00	0.24 (0.07)	0.32(0.10)
Wageningen Univ. (Met)	Vineyard	506009.50, 4332290.00	0.22 (0.11)	0.34 (0.08)
Wageningen Univ. (Wat)	Fallow	508919.50, 4333460.00	0.32 (0.12)	0.32 (0.08)
Copenhagen University	Vineyard	506399.50, 4330940.00	0.17 (0.02)	0.31 (0.12)
Berlin University	Field 2	533189.50, 438680.00	0.58 (0.07)	0.56 (0.28)
Berlin University	Field 3	533369.50, 4380560.00	0.32 (0.12)	0.69 (0.16)
Copenhagen University	Sunfl.	534149.50, 4378490.00	0.27 (0.03)	0.65 (0.13)

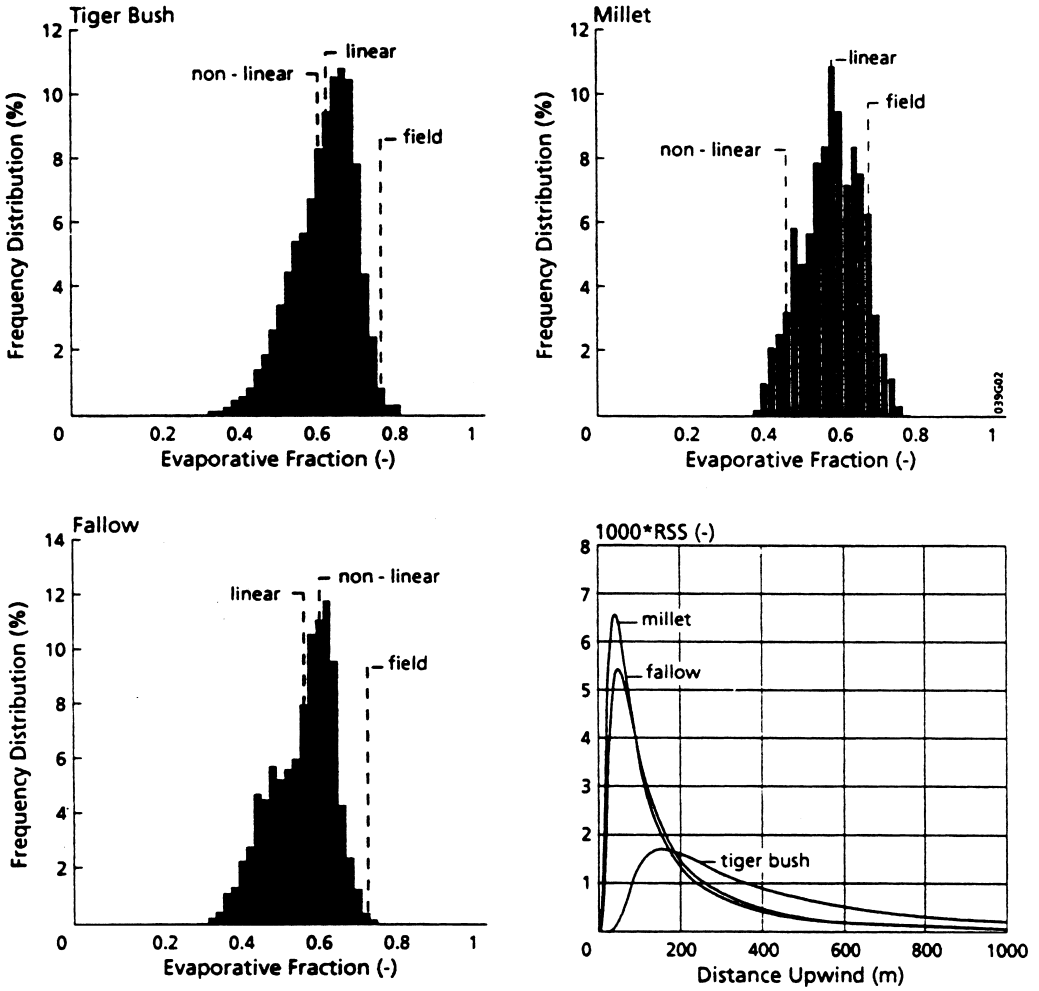

Fig. 5. Area variation in evaporative fraction within the footprint of an individual flux tower. Part A: Tiger bush, Part B: Millet, Part C: Fallow Savanah and Part D: Weighing scheme for the non-linear integration of the upwind fluxes for each individual flux tower where RSS is Relative Source Strength.

estimated as an average of 1425 m for the 13 stations. The hight of the eddy correlation systems varied between 10 and 25 m.

Of the 13 stations, 4 were situated outside the envelope based on one time the standard deviation. As such, the algorithm's performance was not as good as it was for the NS001 images. The root mean square error relative to the centre of the error bar was also much larger: $\Lambda_{\mathrm{RMSE}} = 0.19$. The bulk behaviour of a larger area encompassing all 13 footprints yielded $\Lambda^{\mathrm{eff}}_{\mathrm{Tower}} = 0.45$ while SEBAL gave $\Lambda^{\mathrm{eff}}_{\mathrm{SEBAL}} = 0.49$, indicating that the overall SEBAL performance improves for a larger set of heterogeneous land surface elements ($\Delta\Lambda^{\mathrm{eff}}/\Lambda^{\mathrm{eff}} = 0.94/0.45 = 0.10$).

2.4 Thematic mapper measurements at sahel (HAPEX)

The success of predicting the atmospheric circulation processes over the Sahel is greatly affected by the description of the land surface fluxes (Xue and Shukla, 1990). An intensive international expedition was organized in the autumn 1992 to measure the fluxes from these scattered natural bushlands

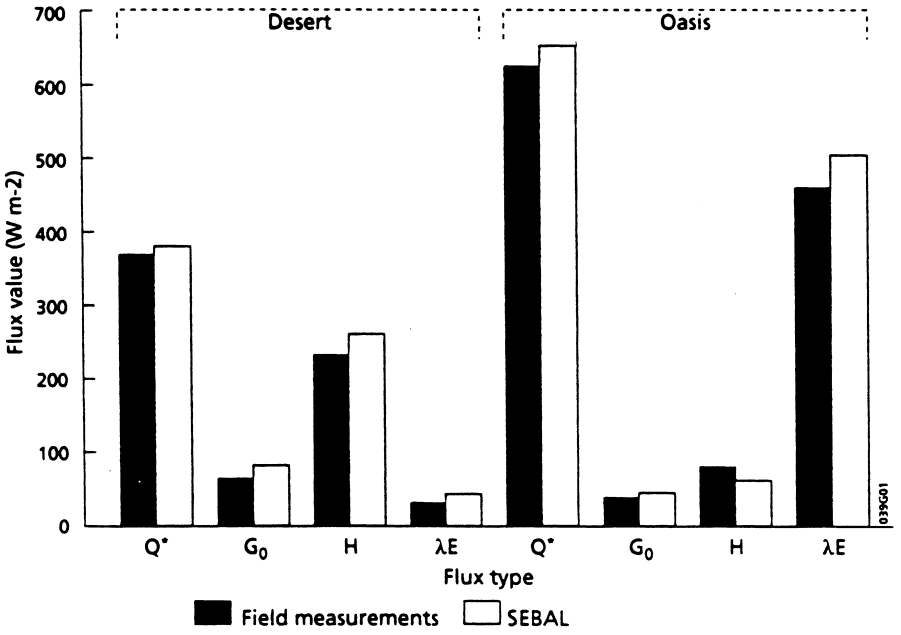

Fig. 6. Measured and SEBAL estimated surface energy balances in a desert-oases system on July 9, 1991, in the Heihe river basin, Gansu, China.

(Goutorbe et al., 1994). September 14 and 15 were rainy days. Application of SEBAL for this region on September 18, 1992, as 2 to 3°E and 13 to 14°N (see Fig. 12) led to the conclusion that a difference of $\Lambda_{RMSE} = 0.14$ between Λ_{SEBAL} and *in-situ* measurements of Λ was unavoidable (Kabat et al., 1997). The equivalent relative error then becomes $\Delta\Lambda/\Lambda^{eff} = 0.20$. This conclusion, was, however, based on3 flux stations only, which is insufficient to draw general conclusions. Fig. 5 shows the frequency distribution of the fluxes withinthe footprint of the flux towers placed in tiger bush, millet and fallow savannah. The effect of linear and non-linear averaging especially affected the millet field, while the tiger bush and fallow savannah were less sensitive to the flux weighing procedure. Each tower had different integration lengths, vis. 6200, 1650 and 2000 m for tiger bush, millet and fallow savannah, respectively. Gash et al. (1997) thoroughly analysed the flux measurements on September 17 (one day before Thematic Mapper overpass) and their data were included in the current validation procedure because of the larger number of stations ($n = 11$). SEBAL estimates $\Lambda^{eff} = 0.57$ for the West Central SAupersite and $\Lambda^{eff} = 0.63$ for the whole TM scene. The 11 flux stations gave on average $\Lambda = 0.66$ for millet, $\Lambda = 0.79$ for fallow savannah and $\Lambda = 0.76$ for patterned woodland. The systematic deviation with remote sensing based estimates of Λ can be explained by the rapid soil moisture depletion of coarse and bare sands between September 17 and 18.

2.5 Thematic mapper measurements of the Heihe river basin (HEIFE)

The Heihe river basin, located at 100°E and 39°N in the gansu Province in the North-western part of the People's Republic of China, has been the focus of a special research programme on the water and energy cycle between mountains, oases and desert since 1988. This HEIFE project (Mitsuta, 1994) involves permanent observations of essential hydro-meteorological parameters dispersed across the area and includes regular field campaigns in which surface fluxes are measured with eddy correlation devices. Basically, the flux stations have been set up in a toposequence going from the irrigated oases fed by water

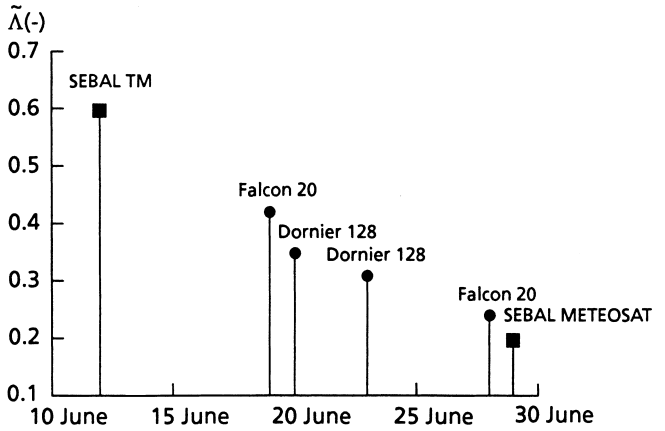

Fig. 7. Temporal behaviour of the aggregated evaporative fraction Λ^{eff} for the entire 900,000 ha EFEDA grid according to SEBAL and aircraft flux measurements made Falcon 20 and Dornier 128.

from the Heihe river, via sand desert to a stony desert surface (Gobi type of desert surface). SEBAL was tested with a Thematic Mapper image of July 9, 1991 (Wang et al., 1995, Ma, 1996) with the aim to extrapolate point measurements obtained. Field data of hemispherical surface reflectance and surface temperature were used to atmospherically correct the spectral radiance's measured by a satellite situated at the top of the atmosphere. Some estimates of surface roughness (z_{0m}) on the basis of wind profile measurements ($u(z)$) were used to fit the emperical relationship between z_{0m} and NDVI. The areal distribution of the latent heat flux is depicted in Fig. 13. The fluxes resulting from SEBAL were compared afterwards with corresponding values measured at ground level (Fig. 6). As the figure shows the soil heat flux gave the poorest results. This was not considered a serious problem, because microscale soil heat flux measurements are representative for a very small sphere of influence and therefore incompatible with the size of one TM-pixel anyhow. Since field measurements of Q^*, G_0, H and λE all have different footprints, the energy budget from measurements in composite terrain is seldom neutral. hence, the results in Fig. 6 for complex terrain conditions should, with an average RMSE of 23 W m^{-2}, be perceived as encouraging. The difference of 25 W m^{-2} in latent heat flux is equivalent to a relative error of 25/244 = 10% which, for one single footprint, is within the range of uncertainty of the field instruments.

3. Validation by means of airborne turbulent flux measurements

3.1. Iberian peninsula, using NOAA-AVHRR and METEOSAT measurements (EFEDA)

A description of macro scale surface energy balances of the entire Iberian Peninsula was obtained by retrieving surface temperature T_0 and hemispherical surface reflectance r_0 from METEOSAT and NDVI from NOAA-AVHRR. Since the METEOSAT flux maps cannot be compared with field measurements directly (pixel size larer than footprint, see Fig. 1), a comparison with aircraft flux measurements has been worked out.

The DLR Falcon 20 aircraft was flown in the EFEDA study area on June 19, 21, 25 and 28, 1991. Eddy correlation apparatus were onboard the aircraft to measure H and λE fluxes at flighing altitude. This independent data source was used to validate a set of 520 METEOSAT pixels covering the EFEDA grid square. The flight pattern on June 28 consisted of parallel legs to obtain the horizontal variability of the fluxes at 350 m height across the full EFEDA domain (Jochum et al., 1993; Jochum, 1993). As the spatial patterns of fluxes change with height, aircraft fluxes cannot be compared with surface fluxes resulting from remote sensing. Instead, evaporative fraction, Λ, of an area can be taken. The average evaporative fraction, based on linear averaging of the H and λE fluxes for legs ML1, ML2, ML4, ML6

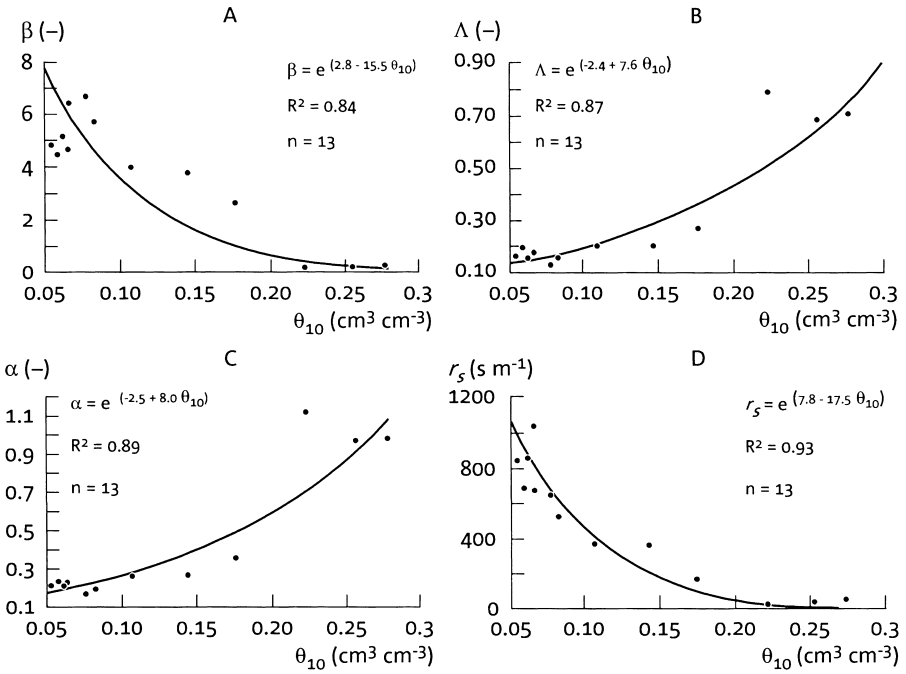

Fig. 8. Non-linear trend between wetness indicators and volumetric soil water content at a depth of 10 cm (Θ_{10}) for Tomelloso and Barrax, enclosing a range of surfaces (vineyard, vetch, bare soil, maize, barley, alfalfa) and soils (reddish sandy loam, loamy sand, limestone) with different soil moisture conditions (0.05–0.30 $cm^3\ cm^{-3}$): Bowen ration β (part A), evaporative fraction Λ (part B), Priestly and Taylor α (part C), bulk surface resistance (part D)), June 29, 10:21 h GMT.

and ML7 was calculated as $\Lambda^{eff}_{Falcon} = 0.24$.The METEOSAT June 29 images for an area of 85 km ∗ 125 km covering almost the entire EFEDA grid yielded an average of $\Lambda^{eff}_{Meteosat} = 0.21$. Since the zone around the Embalse de Alarcon reservoir contributes significantly to $\langle \lambda E \rangle$ and is not including the spatial integration of $\lambda E(x,y)$ because of clouds above the reservoir, the $\Lambda^{eff}_{Meteosat}$-value should be slightly higher, approaching the Falcon $\Lambda^{eff} = 0.24$ value rather closely ($\Lambda^{eff}_{meteosat} - \Lambda^{eff}_{Falcon} \sim 0.0$ to 0.02). Fig. 7 shows that the rapid changes in Λ^{eff} during the course of June from airborne turbulent flux measurements. The SEBAL calculations agree rather well with this trend which indicates that Λ^{eff} of a watershed can be accurately assessed from meteorological satellites. The same conclusion was drawn by van den Hurk et al. (1997) for the evalorative conditions of the entire Iberian Peninsula using synoptical stations for screen light air temperature and air humidity.

4. Validation by means of soil moisture profiles measured in the field

In addition to ground observations of surface fluxes, a soil moisture monitoring programme was executed during EFEDA (Droogers et al., 1993). The energy partitioning in arid conditions relates primarily to near-surface soil water content (e.g. Owe and Van de Griend, 1990). Information on the regional distribution of soil moisture must therefore match the partitioning between H and λE. Four common expressions for energy partitioning or 'wetness indicators', derived from SEBAL output, have been compared with field scale near-surface soil moisture measurements: Bowsen ratio β, Priestley and Taylor α, evaporative fraction Λ and bulk surface resistance, r_s. The relationship between these wetness indicators and the near-surface soil water content provides another yardstick to check

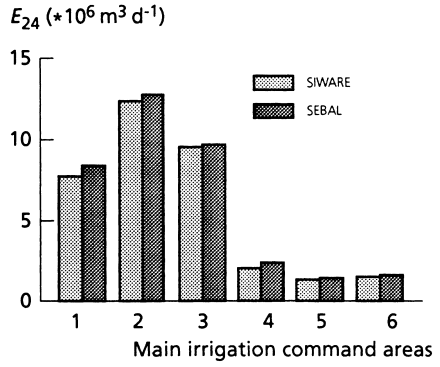

Fig. 9. Relative difference in daily evaporation between SIWARE and SEBAL for the six main irrigation ommand areas. The numbers represents the (1) Ismaileya, (2) Rayah Tawfiki, (3) Mansureya, (4) Sharqaweya, (5) Bassoseya and (6) Abu Managa areas.

the reliability of Λ or λE maps. The measurements of the Time Domain Reflectometer (TDR) reflect the moisture situation of one particular pixel.

Over 46 plots and 13 test fields (some fields include more than one plot), soil mosture was monitored at several standard depths between 5 and 50 cm. Four different test fields were located in the Tomelloso area (vineyard, vetch, bare soil), while the Barrax area included nine test fields (maize, fallow, barley, alfalfa). The incorporation of moisture data in Barrax was particularly valuable, since the surface fluxes in Barrax were available only for three locations (see Table 1). Fig. 8 presents field-averaged moisture

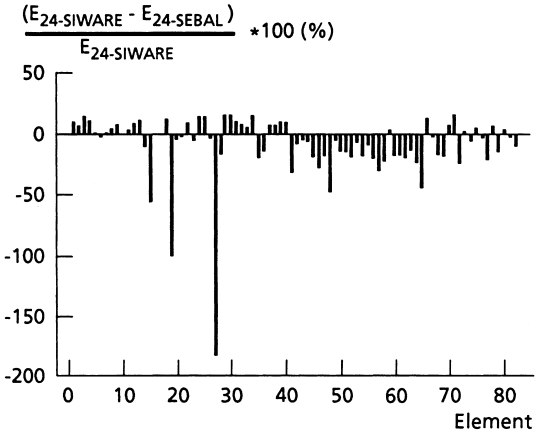

Fig. 10. Determination of the relative deviation $\Delta E/E$ for each of the 82 irrigation units of SIWARE on August 5, 1986. The average value turned out to be $\Delta E/E = -0.08 \pm 0.26$.

conditions at a depth of 10 cm, Θ_{10}, against the SEBAL-derived wetness indicators of that particular field; they compare well. Evidently, r_s shows a better relationship with Θ_{10} than β, α and Λ. There is a well-known non-linearity between the resistance to bare soil evaporation r_{soil} and Θ (Kondo et al., 1990) and between the resistance to crop evaporation r_c and Θ (Jarvis, 1976) for homogeneous surfaces. Fig. 8 allows the conclusion that the non-lienarity between a bulk surface resistance r_s and Θ also holds for *heterogeneous* landscapes (vineyard, vetch, bare soil, maize, barley and alfalfa at different development stages, different soil types and different moisture depletion phases).

5. Validation by means of hydrological models

Apart from aircraft fluxes, a general shortcoming of the validation procedures based on in situ measurements is that only a small number of selected point observations could be used. An alternative way to obtain regional evaporation rates is by studying the water balance of watersheds, river basins or deltas.

5.1. Qattara Depression, using Thematic Mapper measurements (Egypt)

The floor of the 2,000,000 ha vast sub-sea level Qattara Depression in the Westerm Desert of Egypt overlies the fresh water Nubian Sandstone aquifer. Since human activities in this hyper-arid climate without rainfall and runoff are negligible (no groundwater extraction, no crop evaporation) and the phreatic level is stationary throughout the year, the water balance of the Qattara Depression becomes very simple: groundwater inflow is equal to evaporation. Fig. 14 illustrates the general evaporation features estimated with SEBAL in the Eastern part of the Qattara Depression on August 7, 1986. Higher evaporation spots coincide with the locations of the sebkha's and salt marshes where the water table almost reaches the surface.

Numerical groundwater flow models were applied to assess whether estimated groundwater losses by evaporation were consistent with water flow into the depression (Meneti et al., 1991). The model study showed that the SEBAL estimations of evaporation were consistent with the calculated groundwater flow of 2100 $Mm^3\,yr^{-1}$ (FEMSAT model) and

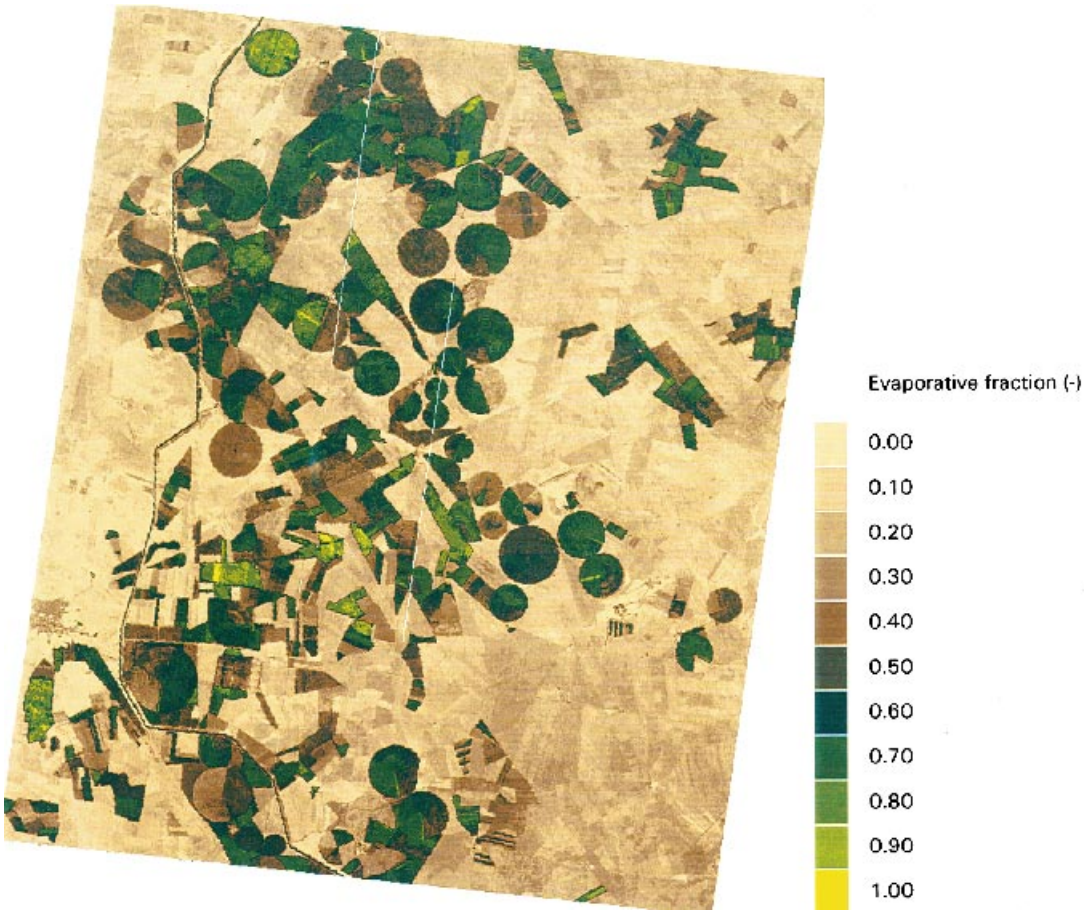

Fig. 11. NS001-based evaporation map for Barrax estimated with the SEBAL parameterization, June 29, 1991. Time integration of instantaneous to 24 hour values was realized by holding evaporative fraction constant and adjust the net radiation.

2300 $Mm^3\ yr^{-1}$ (TRIWACO model) using observed pressure heads and large values for the saturated hydraulic conductivity k_{sat}. Large k_{sat} values, ranging from 300 to 600 cm d^{-1}, could be physically obtained by the lower water viscosity at 60 to 70°C which prevails in deep aquifers (>4000 m).

5.2. Nile Delta, using METEOSAT measurements (Egypt)

Field water balance models usually compute evaporation from vegetation and soil according to the unstressed transpiration and bare soil potential evaporation. Empirical reduction factors based on actual soil water content and salinity, are then applied to correct for less optimal soil moisture and salinity conditions. When this category of models is locally calibrated against soil moisture, groundwater table flucations and return flow, they give reasonable estimates of regional evaporation.

Pelgrum (1992) focussed on the water consumption of the irrigated Nile Delta. An attempt was made to determine the surface energy balance for each daytime hour using METEOSAT-based T_0 and r_0 data. The SEBAL procedure was repeated for each hourly image during daylight (12 images and thus 12 SEBAL runs). A large set of instantaneous surface energy balances between 7 AM and 6 PM was so obtained Feddes et al., 1993). The 24 hour SEBAL evaporation rates obtained for the Nile Delta were

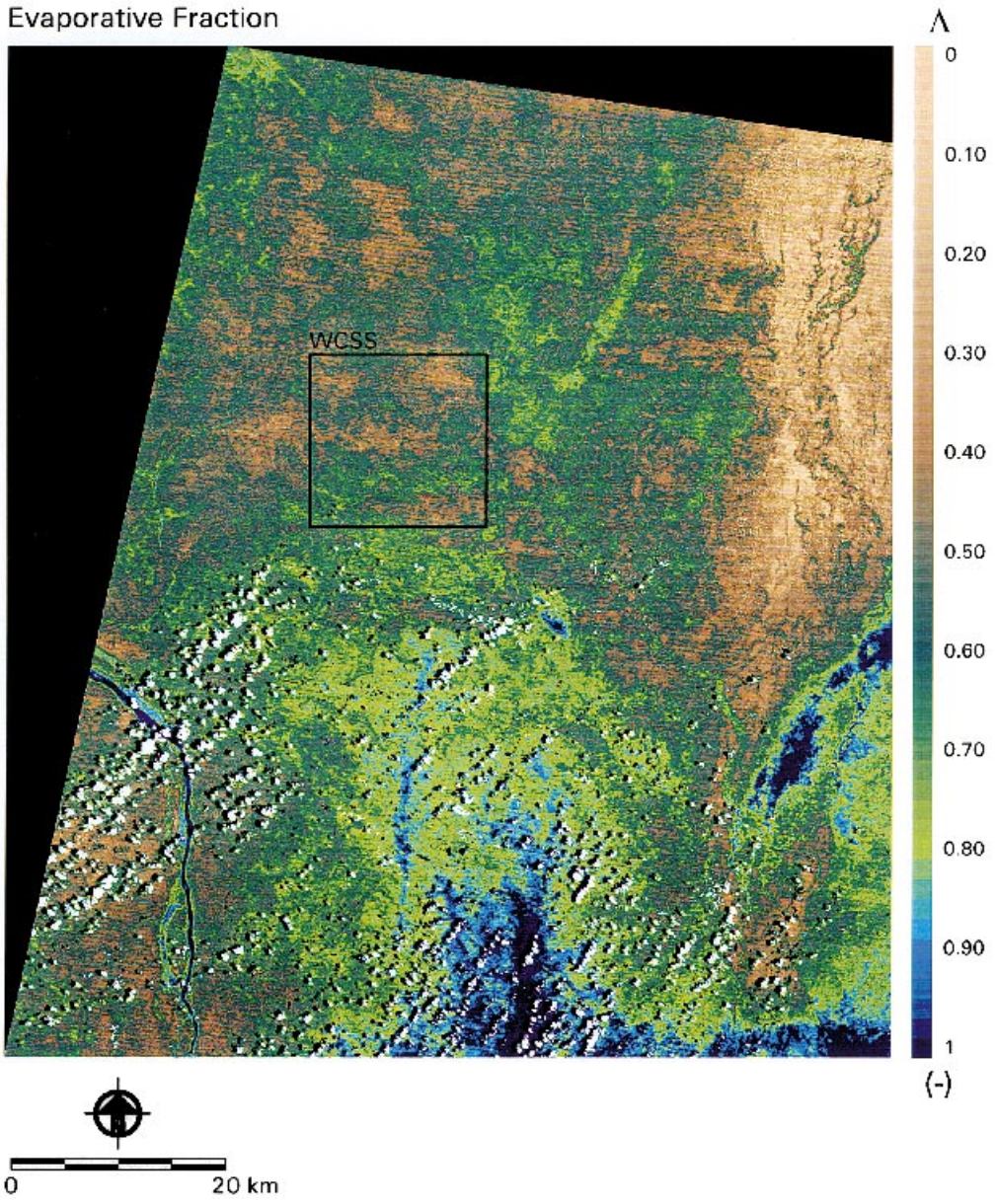

Fig. 12. Thematic Mapper-based evaporative fraction map of the HAPEX-Sahel grid estimated with the SEBAL parameterization, September 18, 1992.

compared by Bastiaanssen et al. (1992) with the 24 hour evaporation figures obtained from the calibrated hydrological model SIWARE (Abdel Gawad et al., 1991). At the time of image acquisition in August 1986, maize, cotton, orchards and vegetables were grown on the irrigated Nile delta. The SIWARE network in the Eastern Nile Delta distincts 82 irrigation units. The total gross irrigated area covered by the 82 irrigation units is 695,000 ha. The results for six irrigation commands are demonstrated in Fig. 9. The relative error of the command areas $\Delta E_{24}/E_{24}$ = (SIWARE-SEBAL)/SIWARE appeared to be

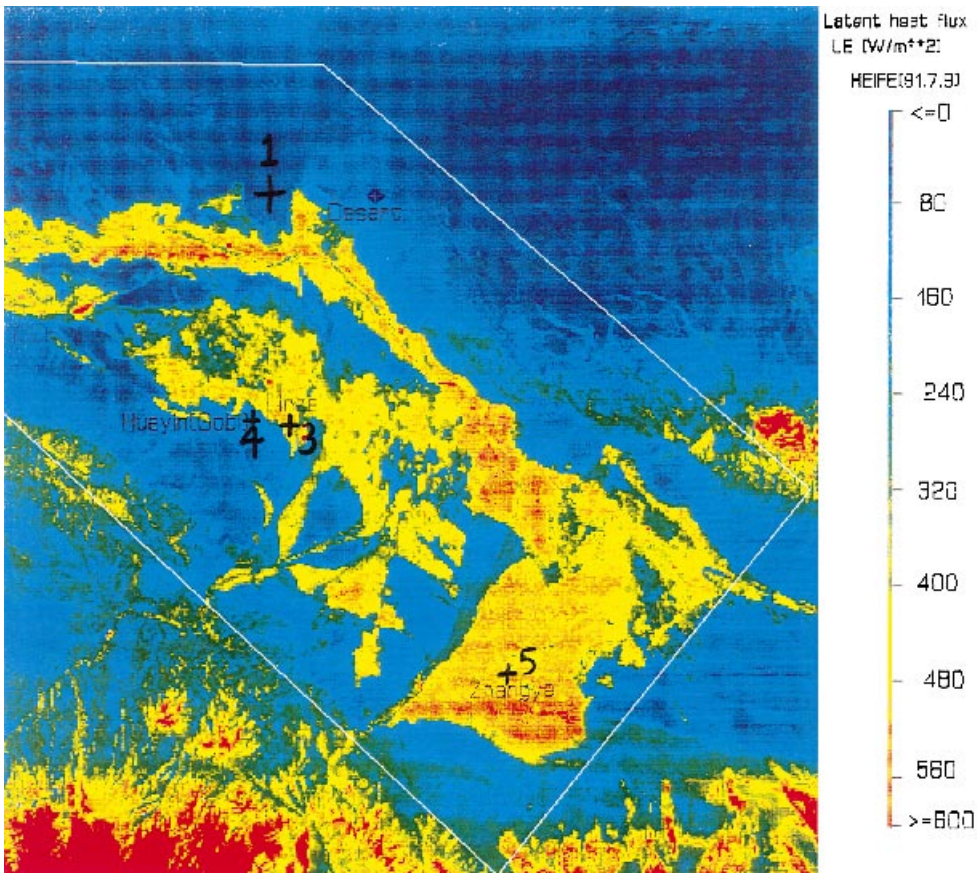

Fig. 13. Thematic Mapper-based latent heat flux map of the Heihe river basin estimated with the SEBAL parameterization, July 9, 1991, 9:50 h local time.

suprisingly small (Fig. 9), with a mean for the 6 cases of $\Delta E_{24}/E_{24} = -0.08$ (SD = 0.06).

A further down-scaling allows extension of the comparative study to the level of each of the 82 irrigation units. The average difference between SEBAL and SIWARE for the individual irrigation units was $\Delta E_{24}/E_{24} = -0.08$ (SD = 0.26). With the exception of units 15, 19 and 27, the results were encouraging (see Fig. 10). For all 82 irrigation units together, daily values of SEBAL were found to be 5.1% higher than the SIWARE predictions. A 5.1% deviation is within the allowable range of the SIWARE model accuracy (10% on an annual basis). Hence, the error in evaporation from remote sensing increases as one goes from extensive composite regions (5.1% deviation) via command areas (8% deviation ± 6%) to isolated irrigation units (8% ± 26%).

6. Summary and conclusions

The five different calibration options all have a certain potential (although groundwater flow models can only be used for a first order estimate; they are just quantitative). Depending on the spatial scale at which the remote sensing study is performed (field, watershed, river basin, continent), a validation procedure can be selected using the summary provided in Table 3.

The difference between tower-based and remote sensing-based Λ-data was found to range from $\Lambda_{RMSE} = 0.10$ to 0.20 for single footprints of several hundreds of metres, independent of land use types (vineyard, bare soil, vetch, irrigated maize, irrigated cotton, sunflower, patterned woodland, millet, Gobi desert and sebkha's). The error is reduced substantially

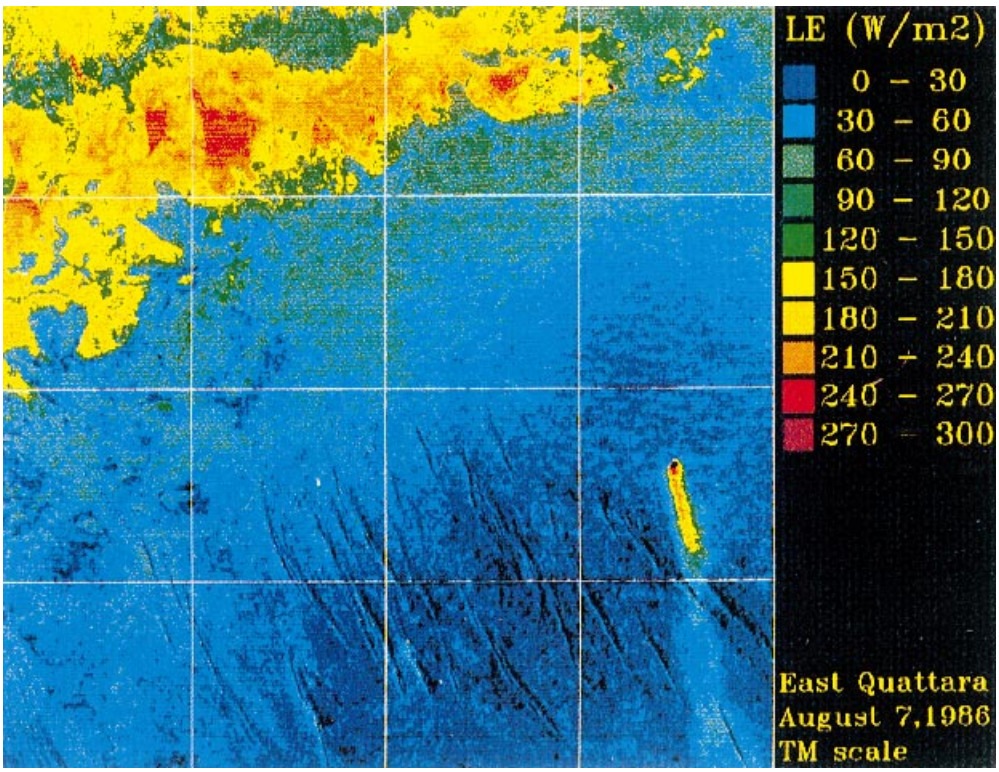

Fig. 14. Thematic Mapper-based latent heat flux map of the Qattra Depression estimated with the SEBAL parameterization and aggregated towards a spatial resolution of 1 km * 1km (NOAA-AVHRR scale), August 7, 1986, 9:50 h local time.

if the individual footprints are areally aggregated to a length scale to a few km ($\Delta\Lambda^{eff} \sim 0.05$). At watershed scale, where aircraft fluxes are meaningful, such as for Castilla la Mancha (1,000,000 ha), the error was $\Delta\Lambda^{eff} \sim 0.01$. For the large areas in the Qattara Depression and Eastern Nile Delta, it was concluded that the evaporation is within the confidence limits of the calibrated water balance models. The validation for natural woodlands such as Rada de Haro and the woodlands in Niger gave moderate results, which in the

Table 3
Evaluation of the validation procedure tested and accuracies obtained for the SEBAL evaporation studies in arid zones

Option	Advantage	Disadvantage	SEBAL Accuracy (%)	Scale (km)
1. Tower fluxes	Direct flux data, field scale	Non-linear averaging of fluxes	85 to 95	0.5 to 5
2. Aircraft fluxes	Direct flux data, large area coverage, regional scale	Expensive, advection, height dependence of fluxes	99	100
3. Soil moisture	Geometric coupling with pixel wise fluxes is easy, field scale	Fluxes are indirectly validated	90	0.5
4. Groundwater models	Physical constraints can be assessed regional scale	Uncertain geo-hydrological schematisation	81	100
5. Field water models	Multi-scale validation feasible regional and field scale	Calibration compulsory for realistic water balances	92 95	10 100

Niger case is most probably related to rapid moisture depletion.

These examples indicate that evaporation assessments from remote sensing data using new type of empirical relationships are feasible with a minimum of collateral input data. SEBAL is not a profitable solution under all circumstances; the attainable accuracy changes with the degree of land surface heterogeneity in relation to pixel size and correlation length of a given landscape (see Bastiaanssen et al., 1996 for more details).

Future large scale field experiments should pay more attention to an exact determination of the footprint orientation and length, in order to calculate the fractional contribution of land surface elements to the total flux measured by the towers. The prospects of long-path scintillometers look promising (De Bruin et al., 1995). The new generation of satellite platforms (Earch Observing System, Envisat) may provide improved measurements of surface roughness, surface emissivity and long wave incoming radiation, which would reduce the number of empirical relatioships currently used by SEBAL.

Acknowledgements

The authors are indebted to Mrs Mieke van Dijk and Mr Bram ten Cate for their careful preparation of the final manuscript while the first author was on leave. The assistance of Dr. Jim Lenahan of the International Water Management Institute at Colombo (Sri Lanka) is respectfully appreciated.

References

Abdel Gawad, S.T., Abdel Khalek, M.A.,Boels, D., El Quosy, D.E., Roest, C.W.J., Rijtema P.E., Smit, M.F.R., 1991. Analysis of water management in the Eastern Nile Delta. Reuse Report 30. DLO Winand Staring Center, Wageningen, The Netherlands. 245 pp.

Bastiaanssen, W.G.M., Pelgrum, H., Droogers, P., de Bruin, H.A.R., M. Menenti, 1997. Area-average estimates of evaporation, wetness indicators and top soil moisture during two golden days in EFEDA. Agr. and Forest Met. 87, 119–137.

Bastiaanssen, W.G.M., Roest, C.W.J. Pelgrum, H., Abdel Khalek, M.A., 1992. Monitoring of the irrigation performance on the basis on actual evapotranspiration: Comparison of satellite data and simulation model results. In: J. Feyen, E. Mwendera and M. Badji (eds). Advances in Planning, Design and Management of Irrigation Systems as Related to Substainable Land use, Center for Irrigation Engineering and ECOWARM, Leuven, Belgium: 473–483.

Bastiaanssen, W.G.M., Pelgrum, H, Meneti, M., Feddes, R.A.,1996. Estimation of surface resistance and Priestley-Taylor α-parameter at different scales. In: J.B. Stewart et al. (eds). Scaling up in hydrology using remote sensing. Institute of Hydrology, Wallingford: 93–111.

Bolle, H.J. and Streckenbach, B., 1992. The ECHIVAL field experiment in a desertification-threatened area EFEDA. First Annual Report to EC.EFEDA-Secretariat, Free University of Berlin, Berlin, Germany.

Bolle, H.J. et al., 1993. EFEDA: European field experiments in a desertification-threatened area. Annales Geophysica 11, 173-189.

de Bruin, H.A.R., van den Hurk, B.J.J.M., Kohsiek, W.,1995. The scintillation method tested over a dry vineyard area. Boundary Layer Met. 76, 25–40.

Chehbouni, A., Lo Seen, D., Njoku, E.G., Lhomme, J.P., Monteny, B., Kerr, Y.H., 1997. Estimation of sensible heat flux over sparsely vegetated surfaces, J. of Hydr. 188–189, 855–868.

Diak, G.R., 1990. Evaluation of heat flux, moisture flux and aerodynamic roughness at the land surface from knowledge of the PBL height and satellite-derived skin temperatures. Agr. and Forest Met. 52, 181–198.

Droogers, P., v.d. Abeele, G.D., Cobbaert, J., Kim, C.P., Rosslerova, R., Soet, M., Stricker, J.N.M., 1993. Basic data sets description and preliminary results of EFEDA-Spain. Report 37. Wageningen Agricultural University Wageningen, Department of Water Resources, Wageningen, The Netherlands.

Feddes, R.A., Menenti, M., Kabat, P., Bastiaanssen, W.G.M., 1993. Is large-scale inverse modelling of unsaturated flow with areal average evaporation and surface soil moisture as estimated from remote sensing feasible? J. of Hydrology, 143, 125–152.

Gash, J.H.C., Kabat, P. et al., 1997.The variability of evaporation during the HAPEX-Sahel Intensive Observation Period. Journal of Hydrology, special issue on HAPEX-Sahel no.188/189: 385–399.

Goutorbe, J.P. et al., 1994. HAPEX Sahel: A large scale study of land-atmosphere interactions in the semi-arid tropics. Annales Geophysicae 12, 53–64.

Gurney, R.J. and Hall, D.J., 1983. Satellite-derived Surface Energy Balance Estimates in the Alaskan Sub-Arctic. J. of Climate and Applied Met., 22, 115–125.

Hurk, B.J.J.M., Bastiaanssen, W.G.M., Pelgrum, H., van Meijgaard, E., 1997. A new methodology for assimilation of initial soil moisture fields in weather prediction models using meteosat and NOAA data. J. of Applied Met. 36, 1,271–1,283.

Itier, B., Brunet, Y., McAnneney, K.J., Lagouarde, J.P., 1994. Downwind evolution of scalar fluxes and surface resistance under conditions of local advection. Part 1: A reappraisal of boundary conditions, Agr. and Forest met. 71, 211–255.

Jarvis, P.G., 1976. The interpretation of the variation in leaf water potential and stomatal conduct ance found in canopies in the field. Phil. Trans. R. Soc. London, Ser. B 273, 593–610.

Jochum, A.M., Michels, B.I., Entstraser, N., 1993. Regional and local variations of evaporation fluxes during EFEDA. Conf. of Hydroclimatology, 17–22 Jan. 1993, Anaheim. 4 pp.

Jochum, A.M., 1993. Evaporation and energy fluxes during EFEDA: horizontal variability are area averaging. In: H.J. Bolle, R.A. Feddes and J. Kalma (eds). Exchange processes at the land surface for a range of space and time scales, IAHS Publ. 212, 373–380.

Kabat, P., Prince, S.D., Prihodko, L., 1997. Hydrologic Atmospheric Pilot Experiment in the Sahel (HAPEX Sahel), Methods, measurements and selected results from the West Central Supersite, Report 130, DLO Winand Staring Centre, Wageningen, The Netherlands, 215–221.

Kondo, J, Saigusa, N., Sato, T., 1990. A parameterization of evaporation from bare soil surfaces. J. Applied Met. 29: 385–389.

Kustas, W.P., Moran, M.S., Jackson, R.D., Gay, L.W., Duell, L.F.W., Kunkel, K.E., Matthais, A.D., 1990.Instantaneous and daily values of the surface energy balance over agricultural fields using remote sensing and reference field in an arid environment. Rem. Sens. Env. 32, 125–141.

Ma, Y., 1996. Regionalization of surface flux densities andseasonal variation in the heterogeneous landscape of HEIFE. Internal Note 422. DLO Winand Staring Centre, Wageningen, The Netherlands. 24 pp.

Menenti, M., Bastiaanssen, W.G.M., Hefny, K., Abd El Karim, M.H., 1991. Mapping of groundwater losses by evaporation in the Western Desert of Egypt. Report 43. DLO Winand Staring Centre, Wageningen, The Netherlands. 116 pp.

Mitsuta, Y.,1994 (ed.). Proc.Int. Symp. on HEIFE. Disaster Prevention Research Institute, Kyoto University, Kyoto, Japan. 722 pp.

Ottle, C., Vidal-Majar, D.D., Girard, R., 1989. Remote sensing applications to hydrological modeling. J. of Hydrology 105, 369–384.

Owe, M., van de Griend, A.A., 1990. Daily surface moisture model for large area semi-arid land application with limited climate data. J. of Hydrology 121, 119–132.

Pelgrum, H.,1992. Mapping areal surface energy balances during daytime using Meteosat data. Internal Note 195. DLO Winand Staring Centre, Wageningen, The Netherlands. 50 pp.

Pelgrum, H., Bastiaanssen, W.G.M., 1996. An intercomparison of techniques to determine the area-averaged latent heat flux from individual in situ observations: a remote sensing approach using EFEDA data. Water Res. Res. 32(9), 2,775–2,786.

Schuepp, P.H., Lecler, M.Y., Mackerson, J.I., Desjardins, R.I., 1990. Footprint prediction of scalar fluxes from analytical solutions to the diffusion equation. Boundary Layer Met. 50, 355–373.

Sellers, P.J., Hall, F.G., 1992. FIFE in 1992: Results, scientific gains and future research directions, Journal of Geophysical Research 97(D17): 19,091-19,109.

Shuttleworth, W.J., R.J. Gurney, A.Y. Hsu and J.P. Ormsby, 1989. FIFE: the variation in energy partitioning at surface flux sites. IAHS Red Book Series no. 186: 67-74.

Smith, R.C.G. and B.J. Choudhury, 1990. Relationship of multispectral satellite data to land surface evaporation from the Australian continent. Int. J. of Remote Sensing 11-11, 2069–2088.

Taconet, O., Bernard, R. Vidal-Madjar, D., 1986. Evapotranspiration over an agricultural region using a surface flux/temperature modelbased on NOAA-AVHRR 5 data. J. of Clim. and Applied Met. 25, 284–307.

Wang, J., Ma, Y., Menenti, M, Bastiaanssen, W.G.M., Mitsuta, Y., 1995. The scaling-up of processes in the heterogeneous landscape of HEIFE with the aid of satellite remote sensing. J. Met. Soc. of Japan 73(6), 1234–1244.

Xue, Y., Shukla, J., 1990. The influence of land surface properties on Sahel climate. J. Climate 6, 2232–2245.